

Epigenetic Modifications Induced by Blimp-1 Regulate CD8⁺ T Cell Memory Progression during Acute Virus Infection

Hyun Mu Shin,^{1,4} Varun N. Kapoor,^{1,4} Tianxia Guan,^{2,3} Susan M. Kaech,^{2,3} Raymond M. Welsh,¹ and Leslie J. Berg^{1,*}

¹Department of Pathology, University of Massachusetts Medical School, Worcester, MA 01655, USA

²Department of Immunobiology, Yale University School of Medicine, New Haven, CT 06520, USA

³Howard Hughes Medical Institute

⁴These authors contributed equally to this work

*Correspondence: leslie.berg@umassmed.edu

<http://dx.doi.org/10.1016/j.immuni.2013.08.032>

SUMMARY

The transcription factor Blimp-1 regulates the overall accumulation of virus-specific CD8⁺ T cells during acute viral infections. We found that increased proliferation and survival of Blimp-1-deficient CD8⁺ T cells resulted from sustained expression of CD25 and CD27 and persistent cytokine responsiveness. Silencing of *Ii2ra* and *Cd27* reduced the Blimp-1-deficient CD8⁺ T cell response. Genome-wide chromatin immunoprecipitation (ChIP) sequencing analysis identified *Ii2ra* and *Cd27* as direct targets of Blimp-1. At the peak of the antiviral response, but not earlier, Blimp-1 recruited the histone-modifying enzymes G9a and HDAC2 to the *Ii2ra* and *Cd27* loci, thereby repressing expression of these genes. In the absence of Blimp-1, *Ii2ra* and *Cd27* exhibited enhanced histone H3 acetylation and reduced histone H3K9 trimethylation. These data elucidate a central mechanism by which Blimp-1 acts as an epigenetic regulator and enhances the numbers of short-lived effector cells while suppressing the development of memory-precursor CD8⁺ T cells.

INTRODUCTION

In response to a virus infection, CD8⁺ T cells proliferate and differentiate into effector cells that eradicate the pathogen. Upon viral clearance, homeostasis is restored and a stable population of virus-specific memory CD8⁺ T cells remains to protect against reinfection by that virus. The quality and quantity of the CD8⁺ T cell response during the initial phase of the primary response governs the frequency and function of long-lived CD8⁺ memory T cells (Obar and Lefrançois, 2010). For an optimal response, CD8⁺ T cells require at least three signals. These include antigenic stimulation through the T cell receptor (TCR), costimulation through receptors such as CD28, CD40, 4-1BB, CD27, ICOS, and/or OX40, and cytokine stimulation via inflammatory cytokines (Duttagupta et al., 2009). The initial TCR engagement triggers the upregulation of costimulatory molecules and cytokine receptors, which are critical for the clonal

expansion and survival of the responding CD8⁺ T cells (Duttagupta et al., 2009). However, this population of CD8⁺ T cells is heterogeneous; the majority of effector cells die, whereas a small population survive and become memory cells (Obar and Lefrançois, 2010). Transcriptional profiling of effector and memory CD8⁺ T cells in models of both acute and chronic virus infection has recently provided insight into the distinct gene expression programs characterizing distinct cell subsets (Doering et al., 2012). Nonetheless, the precise mechanisms by which these transcriptional programs are established and maintained during CD8⁺ T cell differentiation remain largely unknown.

During the past decade, numerous studies have shown that interleukin-2 (IL-2) plays an important role in regulating CD8⁺ T cell responses during the different stages of viral infection (Boyman and Sprent, 2012). In vivo administration of IL-2 during the early stages of the viral response is detrimental to the survival of CD8⁺ T cells; however, IL-2 therapy during the contraction and memory stages of the response promotes CD8⁺ T cell survival (Blattman et al., 2003). Additional studies have indicated that both primary and secondary CD8⁺ T cell responses are impaired in the absence of IL-2 receptor signaling (Mitchell et al., 2010; Williams et al., 2006). CD25, a subunit of the IL-2 receptor, is up-regulated by IL-2 in conjunction with TCR stimulation (Boyman and Sprent, 2012), and at early stages of the response to lymphocytic choriomeningitis virus (LCMV) infection, CD25 expression promotes the development of terminally differentiated effector CD8⁺ T cells (Kalia et al., 2010). Nonetheless, the mechanism by which CD25 expression on CD8⁺ T cells is regulated over the course of the immune response has not been described.

Members of the tumor necrosis factor (TNF) superfamily also contribute to CD8⁺ T cell survival in vivo. CD27, a costimulatory molecule in the TNF receptor family, binds to CD70 and promotes CD8⁺ T cell proliferation (Duttagupta et al., 2009). CD27-deficient mice have decreased primary and secondary CD8⁺ T cell responses to influenza, and CD27 has been shown to be important for the generation of long-term immunity to this infection (Hendriks et al., 2000). CD27 signals also promote survival of activated CD8⁺ T cells by preventing Fas-dependent apoptosis and by inducing the prosurvival factors Bcl2 and BclxL (Dolfi et al., 2008; Peperzak et al., 2010a). A recent study has shown that CD27-CD70 interactions induce IL-2 production and thereby promote clonal expansion of primed CD8⁺ T cells (Peperzak et al., 2010b). CD27 also marks CD8⁺ T cells with memory potential (Hendriks et al., 2000; V.K. and R.M.W.,

unpublished data). However, the mechanism by which CD27 expression on CD8⁺ T cells is regulated during the immune response is not understood.

Blimp-1 is a transcription factor known to regulate the terminal differentiation of numerous cell types (Martins and Calame, 2008). It drives the differentiation of CD8⁺ T cells toward the short-lived effector fate, and the absence of Blimp-1 leads to the development of memory-precursor CD8⁺ T cells that are better at producing IL-2 (Kallies et al., 2009; Rutishauser et al., 2009). Although Blimp-1 is known to regulate a number of target genes mediating plasma cell differentiation (Martins and Calame, 2008), only a few targets of Blimp-1 in CD8⁺ T cells have been identified. One recent study has shown that Blimp-1 directly regulates expression of the DNA-binding inhibitor Id3 and thereby contributes to the development of short-lived effector T cells (Ji et al., 2011). However, more global information on the targets of Blimp-1 in CD8⁺ T cells is currently lacking.

In previously characterized systems, Blimp-1 has been shown to mediate transcriptional repression by associating with histone-modifying enzymes (Ancelin et al., 2006; Gyory et al., 2004; Smith et al., 2011; Su et al., 2009; Yu et al., 2000). Because there is differential histone modification between memory and effector CD8⁺ T cell subsets (Araki et al., 2009), we considered whether Blimp-1 might function in T cells to regulate histone lysine modification. In osteosarcoma and B cell lymphoma cell lines, Blimp-1 recruits the methyltransferase G9a and histone deacetylases HDAC1 and HDAC2 to target genes, leading to repressive modifications such as histone H3-K9 trimethylation and H3 deacetylation, respectively (Gyory et al., 2004; Kubicek et al., 2007; Yu et al., 2000). Whether any of these mechanisms are involved in the Blimp-1-mediated regulation of CD8⁺ T cell differentiation is not known.

We show here that CD25 and CD27 expression is dysregulated in *Prdm1*^{-/-} T cells responding to LCMV infection, that T cells expressing CD25 and CD27 preferentially survive during acute viral infection, that sustained CD25 or CD27 expression by retroviral transduction enhances T cell survival, and that silencing of *Ii2ra* and/or *Cd27* in Blimp-1-deficient CD8⁺ T cells decreases the magnitude of the virus-specific CD8⁺ T cell response. *Ii2ra* and *Cd27* were identified as direct targets of Blimp-1 with the use of deep-sequencing analysis of Blimp-1-bound DNA targets in CD8⁺ T cells (chromatin immunoprecipitation [ChIP] sequencing [ChIP-seq]). At the peak of CD8⁺ T cell expansion, but not early in infection, we show that Blimp-1 binds to regulatory regions of *Ii2ra* and *Cd27* and recruits G9a or HDAC2 to promote repressive histone modifications at these loci. These data provide key insights into the mechanism by which Blimp-1 acts as an epigenetic regulator of target genes, thereby dictating the fate of CD8⁺ effector T cells.

RESULTS

Blimp-1 Suppresses Cytokine Responsiveness of CD8⁺ T Cells at the Peak of the Antiviral Response

To investigate the role of Blimp-1 in regulating CD8⁺ T cell responses during a virus infection, we used mice carrying a conditional *Prdm1* allele in which exon 5 is flanked by loxP sites (Ohinata et al., 2005). This line was crossed to *Cd4-cre*⁺ transgenic mice, thereby deleting *Prdm1* in all αβ T cells, and differed

from those previously used in studies of Blimp-1 function in B and T lymphocytes (Martins et al., 2006; Piskurich et al., 2000). Hereafter, we refer to *Prdm1*^{lox/lox}*xCd4-cre*⁺ mice as “*Prdm1*^{-/-} mice,” *Prdm1*^{lox/lox}*xCd4-cre*⁺ mice as “*Prdm1*^{+/-} mice,” and *Cd4-cre*⁺ littermate controls as “wild-type [WT] mice.” We did not detect any changes in the proportion of lymphocytes in various lymphoid organs (Figure S1A, available online), although naive *Prdm1*^{-/-} mice had a higher proportion of CD44^{hi}CD4⁺ and CD8⁺ T cells (Figure S1B), as previously reported (Kallies et al., 2006; Martins et al., 2006).

Consistent with previous studies (Rutishauser et al., 2009; Shin et al., 2009), there was a marked increase in both the number and the proportion of CD8⁺ T cells in *Prdm1*^{-/-} mice at days 7 and 14 after LCMV-Armstrong infection (Figures 1A and 1B). CD44^{hi}CD8⁺ T cells and LCMV-specific CD8⁺ T cells showed similar increases (Figure 1A). The amount of memory-precursor effector CD8⁺ T cells (MPECs; KLRG1^{lo}IL-7R^{hi}; Joshi et al., 2007) was also higher in *Prdm1*^{-/-} mice than in WT mice at days 7 and 14 postinfection (Figure 1C), consistent with previous data (Rutishauser et al., 2009). Deletion of *Prdm1* in activated CD8⁺ T cells from *Prdm1*^{-/-} mice was confirmed at days 7 and 14 after LCMV infection (Figure S1C). Viral clearance in the spleen was normal in *Prdm1*^{-/-} mice (Figure S1D), indicating that the increased magnitude of the CD8⁺ T cell response to LCMV in *Prdm1*^{-/-} mice was not due to impaired viral clearance. As shown by decreased TUNEL reactivity (Figure 1D), we also found that CD44^{hi}CD8⁺ T cells from LCMV-infected *Prdm1*^{-/-} mice were less apoptotic than those from WT mice at day 9 after LCMV infection, in accord with increased expression of the pro-survival factor Bcl2 at day 7 postinfection (Figure 1E). The transcription factor eomesodermin (EOMES) promotes persistence of memory CD8⁺ T cells (Banerjee et al., 2010). Consistent with this, we found that more virus-specific CD8⁺ T cells from *Prdm1*^{-/-} mice than from WT controls expressed EOMES at days 7 and 14 postinfection (Figure S1E).

Next, we tested the hypothesis that differential expression of cytokine receptors in WT versus *Prdm1*^{-/-} cells contributes to altered T cell survival and/or proliferation. First, CD8⁺ T cells were isolated from WT mice infected with LCMV Armstrong at day 5 (early expansion), day 7 (peak expansion), and day 9 (contraction) postinfection, labeled with CFSE, and cultured in vitro for 2 days with a panel of cytokines (Figure 1F). When isolated at day 5 postinfection, CD8⁺ T cells spontaneously proliferated in the absence of any cytokine; this response was dramatically diminished by day 9 postinfection. In addition, cells isolated at day 5 postinfection showed enhanced proliferation in response to exogenous IL-12, as well as to the common γ chain (γc) family of cytokines, IL-2, IL-4 and IL-15. This response was also attenuated by day 9 postinfection. In contrast, compared to *Prdm1*^{+/-} and WT T cells, *Prdm1*^{-/-} cells had a dramatically enhanced proliferative response to the cytokines IL-2, IL-12, and IL-15 at day 7 postinfection (Figure 1G).

Because the cytokine responsiveness of T cells during viral infections can be regulated by the modulation of cytokine receptor expression (Kalia et al., 2010; Sarkar et al., 2008), we further examined the expression of CD25 (IL-2Rα), CD122 (IL-2Rβ or IL-15Rβ), and CD124 (IL-4Rα) on CD8⁺ T cells at various time points after LCMV infection. Consistent with the functional data (Figure 1F), CD25 and CD122 protein and mRNA expression

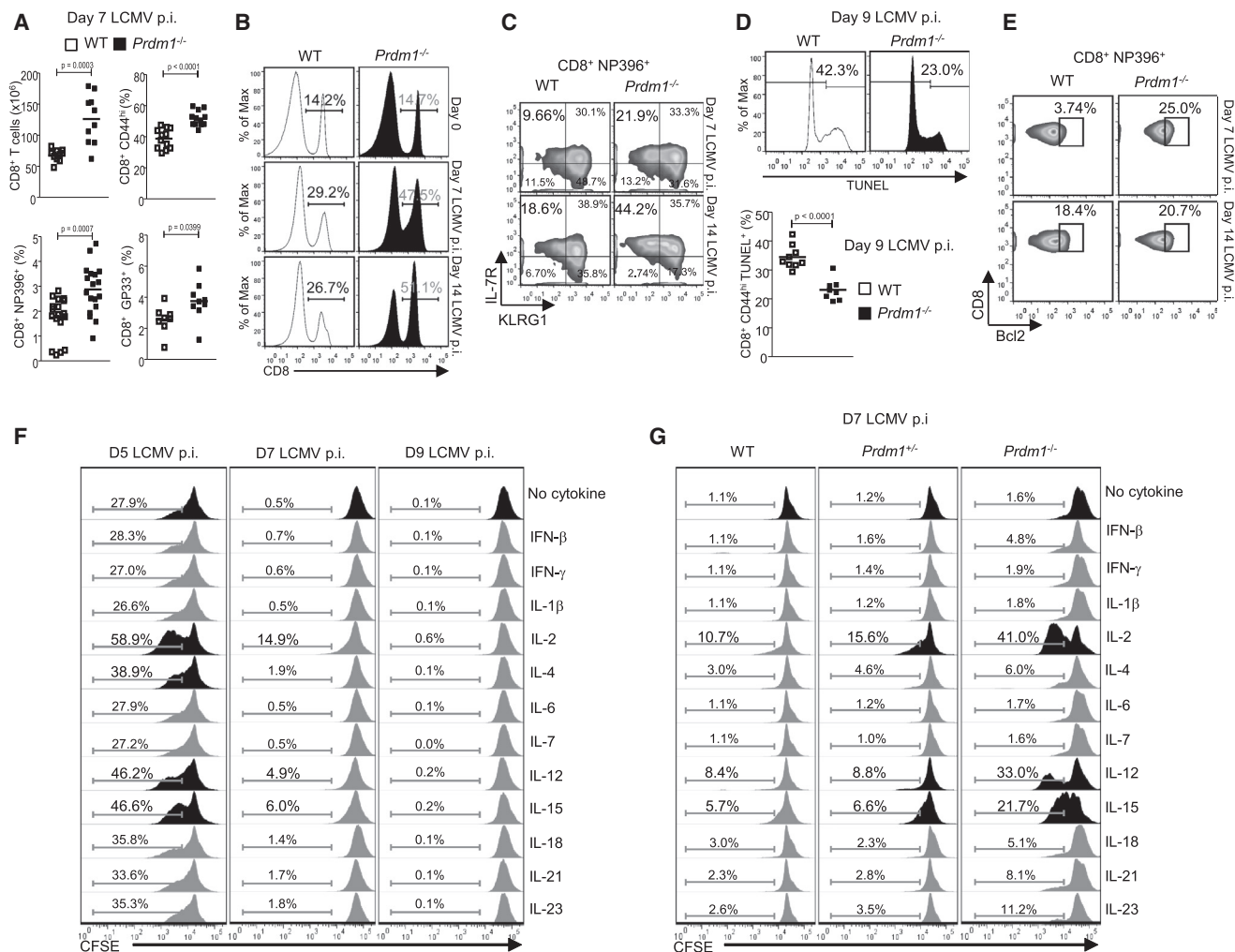


Figure 1. Sustained Cytokine Responsiveness in *Prdm1*^{-/-} CD8⁺ T Cells after LCMV Infection

(A) The total number of CD8⁺ T cells and frequencies of CD8⁺CD44^{hi}, GP33⁺CD8⁺, and NP396⁺CD8⁺ T cells at day 7 after LCMV infection are shown for WT and *Prdm1*^{-/-} mice.

(B) The proportion of total CD8⁺ T cells in LCMV-infected WT and *Prdm1*^{-/-} mice at days 7 and 14 postinfection is shown relative to that in uninfected mice (D0). Histograms are representative of three independent experiments.

(C) NP396 tetramer-binding CD8⁺ T cells in WT and *Prdm1*^{-/-} mice were analyzed for IL-7R and KLRG1 expression at days 7 and 14 after LCMV infection. The numbers indicate the percentage of NP396 tetramer-binding CD8⁺ T cells in each subset. Data are representative of three independent experiments.

(D) Histograms show representative results of TUNEL staining in WT and *Prdm1*^{-/-}CD8⁺CD44^{hi}CD8⁺ T cells at day 9 after LCMV infection. The graph shows a compilation of data from three independent experiments.

(E) NP396 tetramer-binding CD8⁺ T cells in WT and *Prdm1*^{-/-} mice were analyzed for intracellular Bcl2 expression at days 7 and 14 after LCMV infection. The numbers indicate the percentage of Bcl2⁺ T cells in each sample. Data are representative of three independent experiments.

(F and G) CD8⁺ T cells were isolated from (F) WT mice at days 5, 7, and 9 after LCMV infection or from (G) WT, *Prdm1*^{+/-}, or *Prdm1*^{-/-} mice at day 7 postinfection. Cells were labeled with CFSE and cultured for 2 days with or without the indicated cytokines. Numbers indicate the percentage of divided cells. Histograms are representative of three independent experiments.

See also Figure S1.

peaked at day 5 postinfection and then diminished over time through day 9 (Figures S1F and S1G). A similar pattern was seen for *Il12rb1* and *Il12rb2*, the transcripts encoding the subunits of the IL-12 receptor. In contrast, CD124 was expressed in the naive CD8⁺ T cells, and both the protein and mRNA were downregulated after LCMV infection, even at day 5 (Figures S1F and S1G). Compared to WT control cells, *Prdm1*^{-/-} CD8⁺ T cells exhibited increased expression of *Il2ra* mRNA and, to a lesser extent, *Il12rb2* mRNA (Figure S1H). Overall, these data

suggest that decreased responsiveness to cytokines by WT CD8⁺ T cells is due to cytokine receptor downregulation and that Blimp-1 might function to suppress cytokine receptor expression during the antiviral immune response.

Blimp-1 Regulates CD25 Expression in Virus-Specific CD8⁺ T Cells during the Antiviral Immune Response

To test whether CD25 expression was dysregulated in CD8⁺ T cells lacking Blimp-1, we infected WT and *Prdm1*^{-/-} mice

with LCMV and analyzed virus-specific CD8⁺ T cells at days 7–9 postinfection. At day 7, approximately twice as many *Prdm1*^{−/−} T cells as WT T cells expressed CD25 (Figures 2A and 2B). This trend persisted through day 9 postinfection, although the overall proportion of CD25⁺CD8⁺ T cells diminished dramatically after day 7. This function of Blimp-1 was intrinsic to the CD8⁺ T cells, given that a similar difference in CD25 expression was seen in P14 TCR transgenic WT or *Prdm1*^{fllox/flox}*xGzmb-cre*⁺ CD8⁺ T cells (in which Cre expression was under the control of the human Granzyme B promoter [Rutishauser et al., 2009]) responding to LCMV after adoptive transfer into WT congenic hosts (Figure 2C). To further confirm the inverse correlation between Blimp-1 and CD25 expression, we infected Blimp-1-GFP mice, in which GFP expression is under the control of *Prdm1* (Kallies et al., 2006). At days 7 and 9 postinfection, a high proportion of CD44^{hi}CD8⁺ T cells expressed Blimp-1; further, there was an increased proportion of CD25⁺ cells in the Blimp-1^{lo} versus the Blimp-1^{hi} subset (Figure 2D). These data together indicate that Blimp-1 represses CD25 expression at late stages during the antiviral CD8⁺ T cell response.

Recent studies have demonstrated that CD25 expression during the early expansion phase of the antiviral CD8⁺ T cell response is critical in regulating cell fate in that CD25^{hi} cells become short-lived effector cells (Kalia et al., 2010; Pipkin et al., 2010). Consistent with these data, we also observed that high CD25 expression at day 5 postinfection correlated with decreased IL-7R and CD62L expression (Figure 2E); further, at this stage of the response, cells expressing higher Blimp-1 also expressed more CD25 (Figure 2D) (Kalia et al., 2010). These data indicate that strong IL-2R signaling during the early stage of the antiviral CD8⁺ T cell response promotes the development of short-lived effector cells. However, we considered whether the role of IL-2R signaling might be different at the later stage of the response, at which time CD8⁺ T cells undergo attrition. In support of this possibility, we found that at day 9 postinfection, CD25 expression on CD8⁺ T cells positively correlated with IL-7R and CD62L expression (Figure 2E), indicating that compared to the CD25^{lo} population, the CD25^{hi} population at this stage was enriched with memory-precursor cells. Based on KLRG1 and IL-7R expression, analysis of virus-specific CD8⁺ T cells also showed higher expression of CD25 on both KLRG1^{hi}IL-7R^{lo} and KLRG1^{lo}IL-7R^{hi} populations from the *Prdm1*^{−/−} mice than on those from WT controls (Figures S2A and S2B).

To directly test whether differences in CD25 expression on virus-specific CD8⁺ T cells are associated with differences in T cell survival, we sorted CD25^{hi} and CD25^{lo} P14 TCR transgenic CD8⁺ T cells from mice at day 7 after LCMV infection. Sorted T cells were adoptively transferred into infection-matched congenic hosts, and the number of P14⁺ T cells was assessed at day 15 postinfection (8 days posttransfer). We found that a higher proportion and absolute number of virus-specific CD25^{hi}CD8⁺ T cells than of CD25^{lo} transferred cells survived (Figure 2F). These results indicate that, at day 7 postinfection, CD25 expression on virus-specific CD8⁺ T cells correlated with enhanced survival and/or persistence. To determine whether enhanced proliferation contributed to this effect, we injected LCMV-infected mice with bromodeoxyuridine (BrdU) at day 7 postinfection and analyzed virus-specific CD8⁺ T cells 12 hr later. A higher proportion of CD25^{hi} T cells than of CD25^{lo} cells

exhibited BrdU incorporation in WT and *Prdm1*^{−/−} mice (Figure S2C). Additionally, in response to ex vivo LCMV peptide stimulation at day 8 postinfection, a higher proportion of CD25^{hi}CD8⁺ T cells than of CD25^{lo}CD8⁺ T cells produced interferon- γ (IFN- γ) and IL-2 (Figure S2D), correlating high expression of CD25 with a functional memory T cell response. These data indicate that, following the peak of the CD8⁺ T cell response to LCMV, higher expression of CD25 correlates with enhanced survival of virus-specific T cells.

Blimp-1 Regulates CD27 Expression in Virus-Specific CD8⁺ T Cells

CD27 is a costimulatory molecule that promotes CD8⁺ T cell proliferation and memory generation (Duttgupta et al., 2009; Hendriks et al., 2000). To test whether CD27 expression in CD8⁺ T cells is regulated by Blimp-1, we examined T cells from LCMV-infected WT and *Prdm1*^{−/−} mice. At day 9 postinfection, there was a higher proportion of CD27⁺ virus-specific CD8⁺ T cells in the *Prdm1*^{−/−} mice than in the controls (Figure 3A), consistent with previous reports (Kallies et al., 2009; Rutishauser et al., 2009). This difference was visible at day 7.5 postinfection but increased in magnitude at days 8 and 9 (Figure 3B). As was the case for CD25 expression (Figure 2C), altered CD27 expression was due to a CD8⁺-T-cell-intrinsic role for Blimp-1 (Figure 3C) and was observed in both KLRG1^{hi}IL-7R^{lo} and KLRG1^{lo}IL-7R^{hi} populations (Figures S3A and S3B). As a further correlation, we examined CD8⁺ T cells in LCMV-infected Blimp-1-GFP mice. At day 9 postinfection, Blimp-1^{hi} cells expressed less CD27 than did Blimp-1^{lo} cells (Figure 3D).

A previous study showed that CD27-expressing CD8⁺ T cells represent a functional memory cell pool (Hikono et al., 2007). In order to test whether the CD27⁺CD8⁺ T cells present at day 9 after LCMV infection represent a subset enriched with memory-precursor cells, we examined IL-7R expression on cells with varying CD27 expression and found that increasing amounts of IL-7R correlated with increased CD27 expression (Figure 3E).

Virus-specific P14 CD27^{hi} and CD27^{lo}CD8⁺ T cells were next sorted from mice at day 9 after LCMV infection and were adoptively transferred into infection-matched hosts. When analyzed 7 days later (day 16 postinfection), there was a higher proportion and absolute number of P14 CD8⁺ T cells from the CD27^{hi} subset than of cells from the CD27^{lo} subset (Figure 3F). These data together indicate that Blimp-1 normally represses CD27 expression at late stages of the antiviral CD8⁺ T cell response and thereby contributes to the attrition of effector cells after virus clearance.

CD25 and CD27 Expression Enhances the Survival of CD8⁺ T Cells

To test whether persistent CD25 or CD27 expression has a functional role in promoting CD8⁺ T cell survival during an antiviral immune response, we used retroviral gene transfer to constitutively express CD25 or CD27 in LCMV-specific T cells. P14 TCR transgenic CD8⁺ T cells were stimulated in vitro with LCMV-GP33 peptide, infected with retroviruses, and then transferred into LCMV-infected (day 1 postinfection) recipient mice (Figure 4A). Expression of hCD2 indicated that there was a similar transduction efficiency for each of the retroviral (RV)

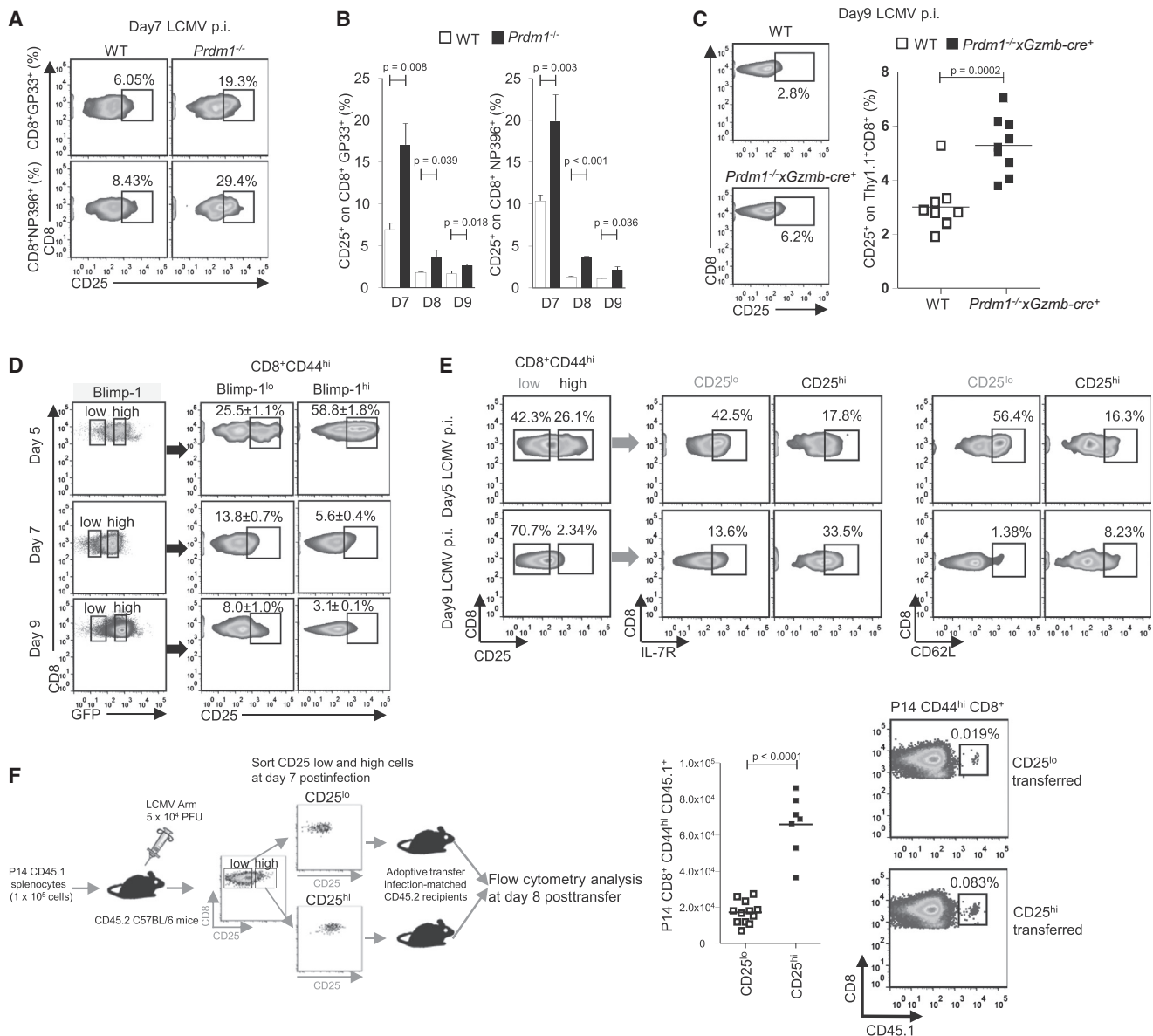


Figure 2. Increased CD25 Expression in *Prdm1*^{-/-} CD8⁺ T Cells during the Antiviral Immune Response

(A and B) CD8⁺ T cells from WT and *Prdm1*^{-/-} mice were isolated at days 7–9 after LCMV infection and stained with CD25 antibodies plus GP33 or NP396 LCMV-specific tetramers. CD25 expression on tetramer-positive CD8⁺ T cells is shown (A) along with a compilation of data from three independent experiments (B). All error bars represent the SEM.

(C) P14 TCR transgenic CD90.1⁺*Prdm1*^{flx/flx}xGzmb-cre⁺ or CD90.1⁺*Prdm1*^{flx/flx}xGzmb-cre⁻ (WT) littermate splenocytes were adoptively transferred into CD90.2⁺ congenic WT mice, and infection with LCMV followed. At day 9 postinfection, CD90.1⁺CD8⁺ T cells were analyzed for CD25 expression (left panels). On the right, the percentages of CD25⁺CD90.1⁺CD8⁺ T cells from two independent experiments each with four to five mice are shown.

(D) Blimp-1-GFP reporter mice were infected with LCMV, and CD44^{hi}CD8⁺ T cells were analyzed at days 5, 7, and 9 postinfection for GFP expression (left panels). On the right, Blimp-1^{lo} and Blimp-1^{hi} populations were analyzed for CD25 expression. The percentages \pm SEM of CD25⁺ cells are indicated on each plot. Data are representative of two independent experiments.

(E) WT mice were infected with LCMV, and CD44^{hi}CD8⁺ T cells were analyzed on days 5 and 9 postinfection for CD25 expression (left panels). On the right, CD25^{lo} and CD25^{hi} populations were analyzed for IL-7R and CD62L expression. The percentages of positive cells are indicated on each plot. Data are representative of four independent experiments.

(F) P14 TCR transgenic CD45.1⁺ splenocytes were adoptively transferred into CD45.2⁺ congenic WT mice, and infection with LCMV followed. At day 7 postinfection, 1 \times 10⁶ CD25^{lo}P14⁺CD45.1⁺CD8⁺ or CD25^{hi}P14⁺CD45.1⁺CD8⁺ T cells were isolated by cell sorting and adoptively transferred into infection-matched CD45.2⁺ recipient mice. Eight days later, P14⁺ cells were assessed. Data shown include a compilation of two independent experiments and representative flow cytometry analysis.

See also Figure S2.

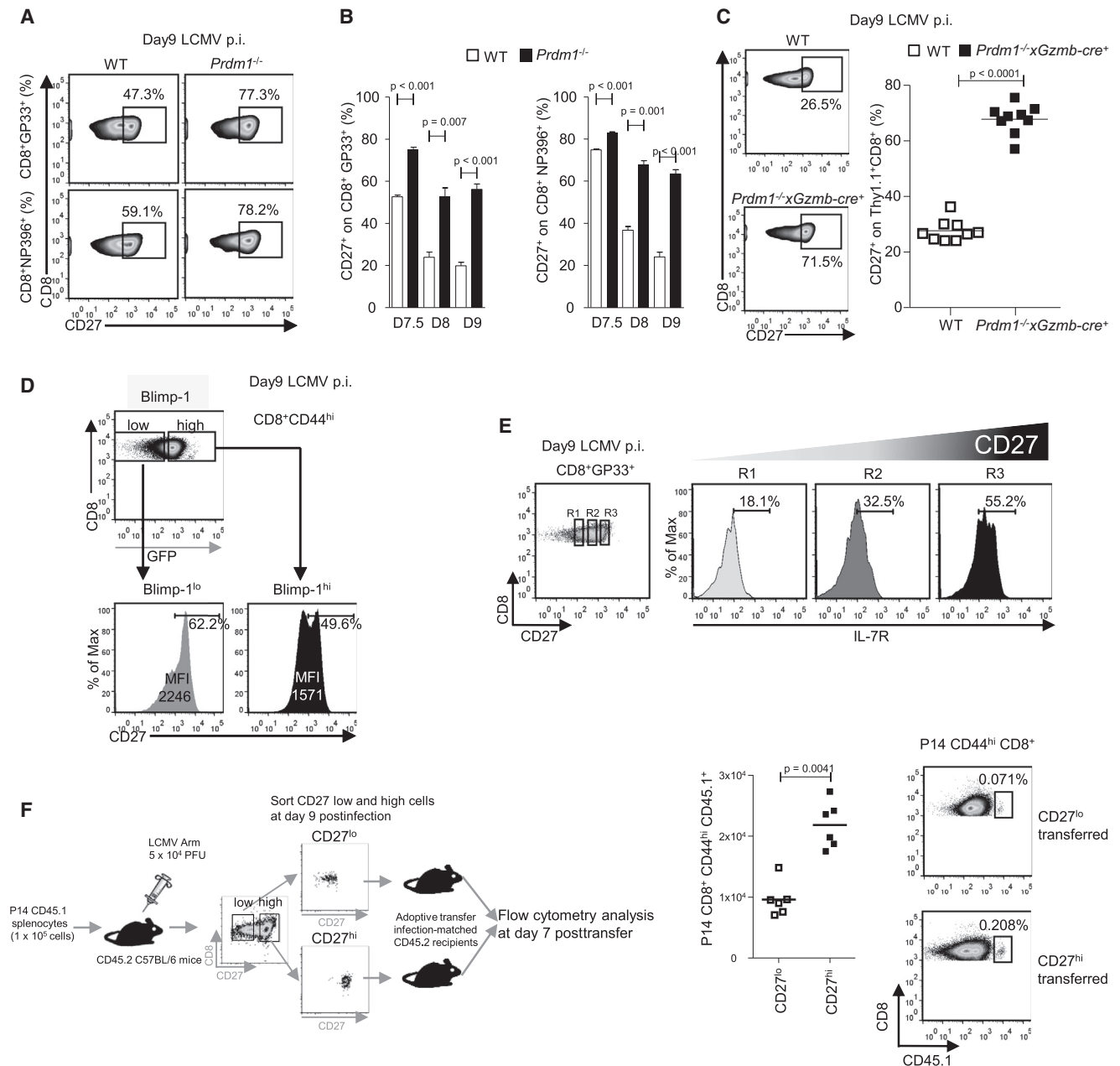


Figure 3. Increased CD27 Expression in *Prdm1*^{-/-} CD8⁺ T Cells during the Antiviral Immune Response

(A and B) CD8⁺ T cells from WT and *Prdm1*^{-/-} mice were isolated at day 9 after LCMV infection and stained with CD27 antibodies plus GP33 or NP396 LCMV-specific tetramers. CD27 expression on tetramer-positive CD8⁺ T cells is shown (A) along with a compilation of data from three experiments (B). All error bars represent the SEM. (C) P14 TCR transgenic CD90.1⁺*Prdm1*^{flx/flx}xGzmb-cre⁺ or CD90.1⁺*Prdm1*^{flx/flx}xGzmb-cre⁻ (WT) littermate splenocytes were adoptively transferred into CD90.2⁺ WT mice, and infection with LCMV followed. At day 9 postinfection, CD90.1⁺CD8⁺ T cells were analyzed for CD27 expression (left panels). On the right, a compilation of data from two independent experiments each with four to five mice is shown. (D) Blimp-1-GFP reporter mice were infected with LCMV, and CD44^{hi}CD8⁺ T cells were analyzed at day 9 postinfection for GFP expression (top panel). Below, Blimp-1^{lo} and Blimp-1^{hi} populations were analyzed for CD27 expression. The percentages of CD27-positive cells and the mean fluorescence intensity of CD27 expression are indicated on each histogram. Data are representative of two independent experiments. (E) WT mice were infected with LCMV, and CD44^{hi}CD8⁺ T cells were analyzed on day 9 postinfection for CD27 expression (left panel). On the right, CD27^{lo} (R1), CD27^{int} (R2), and CD27^{hi} (R3) populations were analyzed for IL-7R expression. The percentages of IL-7R-positive cells are indicated on each histogram. Data are representative of four independent experiments. (F) P14 TCR transgenic CD45.1⁺ splenocytes were adoptively transferred into CD45.2⁺ WT mice, and infection with LCMV followed. At day 9 postinfection, 1 × 10⁶ CD27^{lo}P14⁺CD45.1⁺CD8⁺ or CD27^{hi}P14⁺CD45.1⁺CD8⁺ T cells were isolated by cell sorting and were adoptively transferred into infection-matched CD45.2⁺ recipient mice. Seven days later, the absolute numbers and percentages of P14⁺ cells were determined. Data shown include a compilation of two independent experiments and representative flow cytometry analysis.

See also Figure S3.

constructs; furthermore, compared to mock RV controls, RV transduction led to increased CD25 or CD27 expression (Figure 4B). When analyzed at days 8, 11, and 14 postinfection, LCMV-specific P14⁺ cells expressing either CD25 or CD27 were increased in proportion relative to cells transduced with the empty RV (mock RV; Figures 4C and 4D). These results indicate that persistent CD25 and CD27 expression promotes enhanced expansion of T cells rather than effecting contraction and thereby leads to increased survival of CD8⁺ T cells.

To address whether CD25 or CD27 expression accounts for the enhanced survival of *Prdm1*^{-/-} CD8⁺ T cells during an antiviral immune response, we utilized small hairpin RNA (shRNA) silencing to diminish expression of these proteins in LCMV-specific *Prdm1*^{-/-} T cells. For these experiments, adoptively transferred P14⁺CD90.1⁺*Prdm1*^{fllox/fllox}*xGzmb-cre*⁺ splenocytes were activated in vivo by infection of recipient mice with LCMV. At day 5 postinfection, P14⁺ T cells were isolated by cell sorting, stimulated in vitro with CD3 and CD28 antibodies for 24 hr, infected with retroviruses, and then transferred into LCMV-infected (day 6 postinfection) recipient mice (Figure 4E). As shown, we achieved similar transduction efficiencies for each of the RV constructs (Figure 4F); in addition, each shRNA was able to reduce expression of the targeted gene (Figure 4G). When analyzed at day 9 postinfection, the proportion of *Prdm1*^{-/-} CD8⁺ T cells transduced with shCD25 or shCD27 was lower than that of cells transduced with the scrambled shRNA control (Figures 4G and 4H). Moreover, silencing of both *Il2ra* and *Cd27* further decreased the frequency of GFP⁺CD8⁺ T cells (Figures 4G and 4H). These results indicate that the increased magnitude and survival of CD8⁺ T cells in *Prdm1*^{-/-} mice was in part due to sustained expression of CD25 and CD27.

Genome-wide ChIP-Seq Analysis Identifies *Il2ra* and *Cd27* as Direct Targets of Blimp-1 in CD8⁺ T Cells

Transcriptional regulation by Blimp-1 has been extensively studied in B cells, leading to the identification of *Myc*, *Pax5*, *Bcl6*, *Ciita*, *Spib*, *Id3*, and *Prdm1* as direct Blimp-1 target genes (Martins and Calame, 2008). Substantially less is known about the direct targets of Blimp-1 in T cells, particularly CD8⁺ T cells. To address whether *Il2ra* or *Cd27* might be a direct target of Blimp-1, we performed genome-wide ChIP-seq analysis. Naive CD8⁺ T cells from OT-I TCR transgenic *Rag1*^{-/-} mice were stimulated for 3 days in vitro in the presence of IL-2 to upregulate Blimp-1 (Gong and Malek, 2007) (Figure 5A). For identifying the genomic locations of Blimp-1 binding sites, chromatin was immunoprecipitated with Blimp-1 antibody and DNA was subjected to deep sequencing. The majority of sites identified were located within introns or in regions distal to a gene (49% or 29%, respectively); a minority of binding sites was found in promoter regions (Figure 5B). Using the Ingenuity pathway database, we classified 10,847 Blimp-1 target genes and found that the majority of known genes were in the groups encoding enzymes, transcriptional regulators, transporters, and kinases (Figure S4). To address the functional importance of specific Blimp-1 target genes in CD8⁺ T cells, we chose to focus on cytokine and other transmembrane receptors (Figure 5C and Table S1) because these are known to be critical in regulating T cell function and differentiation. Consistent with previous studies (Ji et al., 2011; Rutishauser et al., 2009), this analysis identified *Prdm1*,

Id3, *Bcl6*, *Pax5*, *Myc*, and *Ciita* as having Blimp-1 binding sites in CD8⁺ T cells (Figure 5D). In addition, we identified *Il2ra*, *Cd27*, *Il2rb*, *Sell* (*Cd62l*), *Eomes*, and *Ccr6* as Blimp-1 targets (Figure 5E). In CD4⁺ T cells, *Il2* is a downstream target of Blimp-1 (Martins et al., 2008); however, we did not detect Blimp-1 binding to the *Il2* locus in CD8⁺ T cells.

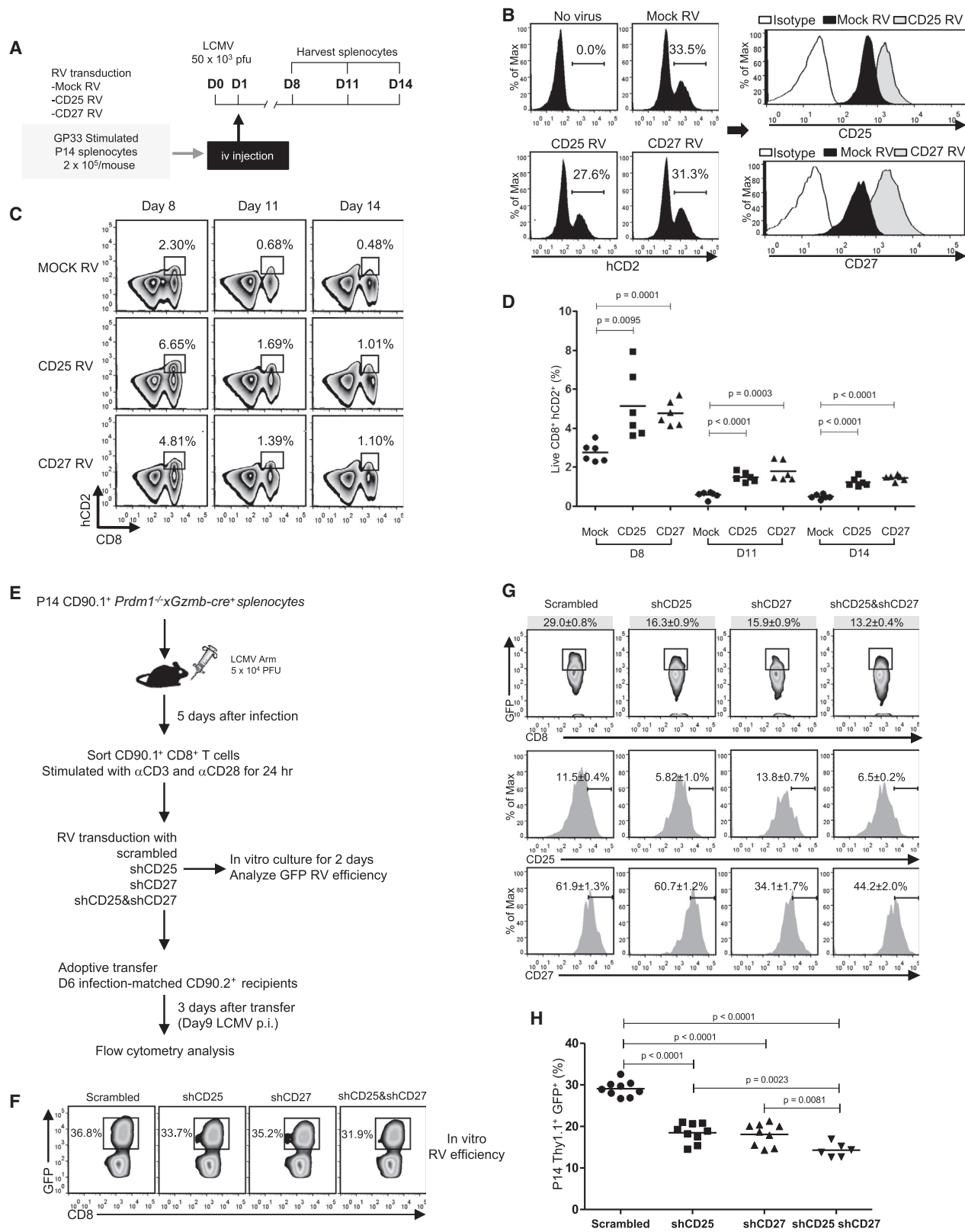
The ChIP-seq analysis identified Blimp-1 binding sites in the first intron of *Il2ra* and at two distal sites within 10 kb of the *Cd27* transcription start site (Figure 5E). When using activated cells from LCMV-infected mice at day 7 postinfection, we found that Blimp-1 bound to the *Il2ra* and *Cd27* loci in WT CD8⁺ T cells (Figure 5F). As expected, there was no binding of Blimp-1 to any of these sites in *Prdm1*^{-/-} CD8⁺ T cells, nor was Blimp-1 binding detected at nonspecific regions (Amp2 in *Il2ra* and Amp3 in *Cd27*). These data support the conclusion that Blimp-1 binding to the *Il2ra* and *Cd27* loci represses expression of CD25 and CD27, respectively, during the antiviral CD8⁺ T cell response.

Blimp-1 Is Associated with Histone-Modifying Enzymes G9a and HDAC2 in CD8⁺ T Cells

To address the mechanism by which Blimp-1 mediates transcriptional repression in primary CD8⁺ T cells, we first performed coimmunoprecipitation assays on T cells activated in vitro. Given that Blimp-1 expression in T lymphocytes requires a combination of TCR plus cytokine stimulation (Gong and Malek, 2007), we compared cells activated through the TCR for 3 days in the presence or absence of a cytokine cocktail containing IL-2, IL-4, and IL-12. Blimp-1 was then immunoprecipitated, and potential binding partners were identified by immunoblotting with antibodies to the histone methyltransferases, G9a or EZH2, or to the histone acetyltransferases, HDAC1 or HDAC2. As shown in Figure 6A, Blimp-1 associated with G9a and HDAC2, but not with HDAC1 or EZH2. Similarly, immunoprecipitates of HDAC2 or G9a coprecipitated Blimp-1, but interestingly, G9a was not associated with HDAC2, indicating that the Blimp-1-HDAC2 and the Blimp-1-G9a complexes are distinct. To confirm these interactions in a more physiological setting, we performed a single-cell-based proximity ligation assay. This assay reveals protein-protein interactions when two protein-antibody complexes are in sufficiently close proximity. Interactions between Blimp-1 and G9a, Blimp-1 and HDAC2, or Blimp-1 and EZH2 were analyzed in situ in activated CD8⁺ T cells by intracellular labeling with each antibody (Figure 6B). These data demonstrate that Blimp-1 and G9a, or Blimp-1 and HDAC2, are within 16 nm of each other in intact nuclei of activated CD8⁺ T cells, thereby supporting a role for Blimp-1 in recruiting these repressive chromatin-modifying enzymes to Blimp-1 target genes in CD8⁺ T cells.

Blimp-1 Promotes Repressive Chromatin Modifications by Recruiting Histone-Modifying Enzymes to Target Genes

To examine whether Blimp-1 mediates the recruitment of histone-modifying enzymes G9a or HDAC2 to Blimp-1 binding sites, we isolated CD8⁺ T cells from WT or *Prdm1*^{-/-} mice at day 7 after LCMV infection. ChIP assays revealed that both G9a and HDAC2 were present at the *Il2ra* and *Cd27* loci in WT CD8⁺ T cells at day 7 postinfection (Figures 7A and 7B). We did not detect binding of G9a or HDAC2 to any of these sites



(legend on next page)

in *Prdm1*^{-/-} CD8⁺ T cells, indicating that Blimp-1 is required for the recruitment of G9a and HDAC2 to these genes. To determine whether Blimp-1 forms a complex with either G9a or HDAC2 at these loci, we performed sequential ChIP assays (ChIP-reChIP) with CD8⁺ T cells from WT or *Prdm1*^{-/-} mice at day 7 after LCMV infection. First, a primary ChIP with Blimp-1 antibody was performed; after elution of these complexes from the primary antibody, secondary immunoprecipitations with G9a or HDAC2 antibody were performed (Figure 7C). These data indicated that Blimp-1 is in close proximity to G9a and HDAC2 on the *Ii2ra* locus. On *Cd27*, Blimp-1 was tightly associated with HDAC2, but association with G9a was weaker at the distal site and absent from the proximal region. Together, these findings provide evidence that Blimp-1 recruits G9a and HDAC2 to target genes in primary T cells activated in vivo.

To determine whether this recruitment is associated with changes in histone modifications at these loci, we examined histone H3 acetylation (H3Ac) and methylation on *Ii2ra* and *Cd27* by ChIP. H3Ac and histone H3 trimethylation on lysine 4 (H3K4me3) are indicative of permissive chromatin states, given that they correlate with gene expression (Weng et al., 2012). In contrast, histone H3 methylation on lysine 9 (H3K9me2 or H3K9me3) and on lysine 27 (H3K27me3) mark repressive chromatin states that correlate with gene silencing (Kouzarides, 2007). Compared to CD8⁺ T cells from WT control mice, CD8⁺ T cells isolated from *Prdm1*^{-/-} mice at day 7 after LCMV infection had increased amounts of H3Ac and H3K4me3 and reduced amounts of H3K9me2, H3K9me3, and H3K27me3 at the *Ii2ra* locus (Figure 7D). Analysis of the *Cd27* locus revealed that compared to WT cells, *Prdm1*^{-/-} CD8⁺ T cells also showed an increase in permissive modifications and a reduction in repressive modifications, although these correlations were not uniformly observed at both of the regions analyzed (Figure 7E). Overall, these chromatin states correlated with the increased CD25 and CD27 expression seen in *Prdm1*^{-/-} versus WT CD8⁺ T cells from LCMV-infected mice.

At day 5 postinfection, Blimp-1 and CD25 were highly expressed, and unlike at day 9 postinfection, their expression levels positively correlated with each other (Figure 2D and Figure 7F). ChIP analysis of the *Ii2ra* locus in CD25^{hi} CD8⁺ T cells isolated at day 5 after LCMV infection showed high amounts of H3Ac in the absence of repressive modifications, along with an absence of Blimp-1, G9a, or HDAC2 binding (Figure 7G). Blimp-1 binding was still detected at one site on *Cd27* at day 5

postinfection, but in this case, Blimp-1 binding was not sufficient to recruit G9a or HDAC2 (Figure 7H), consistent with the lack of repressive modifications and high amounts of H3Ac at this locus (Figure 7I). Together, these findings demonstrate that Blimp-1 induces a repressive chromatin state at *Ii2ra* and *Cd27* in CD8⁺ T cells at the peak of the response to LCMV infection, but not at earlier stages.

DISCUSSION

Prdm1^{-/-} CD8⁺ T cells have an enhanced capacity to differentiate into memory cells (Kallies et al., 2009; Rutishauser et al., 2009). In this report, we have identified an important mechanism by which Blimp-1 association with histone-modifying enzymes suppresses *Ii2ra* and *Cd27* expression to regulate the overall magnitude of the virus-specific memory CD8⁺ T cell response. Upon virus infection and T cell activation, costimulatory signals, along with the inflammatory cytokine milieu, are key components leading to the generation of CD8⁺ effector and memory-precursor T cells that together promote virus clearance and provide long-term protection against reinfection. After virus clearance, CD8⁺ T cells downregulate costimulatory receptor and cytokine receptor expression (Dolfi et al., 2008; Kalia et al., 2010). After this process, the vast majority of the virus-specific effector population undergoes apoptosis (Razvi et al., 1995), most likely as a result of cytokine deprivation and the lack of costimulatory signals. Our data indicate that CD25 (or CD27) has an impact on the small proportion of effector cells capable of long-term survival and provides an important signal to promote the survival of cells expressing the receptor in this specific subset. We propose that Blimp-1 normally functions to downregulate cytokine receptor expression and thereby promotes the death of effector T cells. This mechanism would function in addition to the regulation of proliferation and survival genes by Blimp-1, as proposed previously (Martins et al., 2008).

Over the past decade, numerous studies have investigated the role of IL-2 signaling in CD8⁺ T cell activation and differentiation in response to virus infections (Boyman and Sprent, 2012). These studies showed that CD25 expression and the strength of IL-2R signaling during T cell priming influences the relative generation of effector versus memory CD8⁺ T cells. Furthermore, in vivo administration of IL-2 or IL-15 during T cell contraction increases the size of the CD8⁺ memory pool. These data prompted us to investigate whether IL-2 receptor expression is regulated by

Figure 4. Sustained CD25 and CD27 Expression Extends the Survival of CD8⁺ T Cells

(A) Splenocytes from P14 TCR transgenic mice were stimulated with GP33 peptide for 1 day and then transduced with retroviruses expressing CD25 or CD27 or an empty virus (mock RV) as a negative control. A total of 2×10^5 splenocytes were adoptively transferred into recipient mice 1 day after LCMV infection, and splenocytes from infected recipient mice were analyzed on days 8, 11, and 14 postinfection.

(B) A subset of transduced splenocytes was cultured in vitro for 2 days, and the transduction efficiency was assessed by staining for human CD2 (hCD2). On the right, enforced CD25 or CD27 expression on hCD2⁺ cells was assessed.

(C and D) Representative plots (C) and a compilation of data (D) from two independent experiments show hCD2⁺ CD8⁺ T cells at days 8, 11, and 14 after LCMV infection in recipient mice receiving cells transduced with the indicated retrovirus.

(E) P14 TCR transgenic CD90.1⁺ *Prdm1*^{fllox/fllox} *Gzmb*-cre⁺ splenocytes were adoptively transferred into CD90.2⁺ WT mice, and infection with LCMV followed. At day 5 postinfection, CD90.1⁺ CD8⁺ T cells isolated by cell sorting were stimulated with α CD3 and α CD28 for 24 hr and then transduced with retroviruses expressing shRNAs to silencing *Ii2ra* (shCD25), *Cd27* (shCD27), shCD25, and shCD27 or scrambled as a negative control. Retrovirally transduced cells were adoptively transferred into day 6 infection-matched CD90.2⁺ recipient mice.

(F) A subset of transduced CD90.1⁺ CD8⁺ T cells was cultured in vitro for 2 days, and the transduction efficiency was assessed by GFP fluorescence.

(G and H) Three days after transfer, the percentages \pm SEM of GFP⁺ CD90.1⁺ CD8⁺ cells were determined; dot plots show a representative experiment (G, top panel), and a compilation of data from three independent experiments is shown as a scatter plot (H). A representative example of CD25 and CD27 expression on GFP⁺ CD90.1⁺ CD8⁺ cells, along with the percentages \pm SEM from three compiled independent experiments, is shown (G, lower panels).

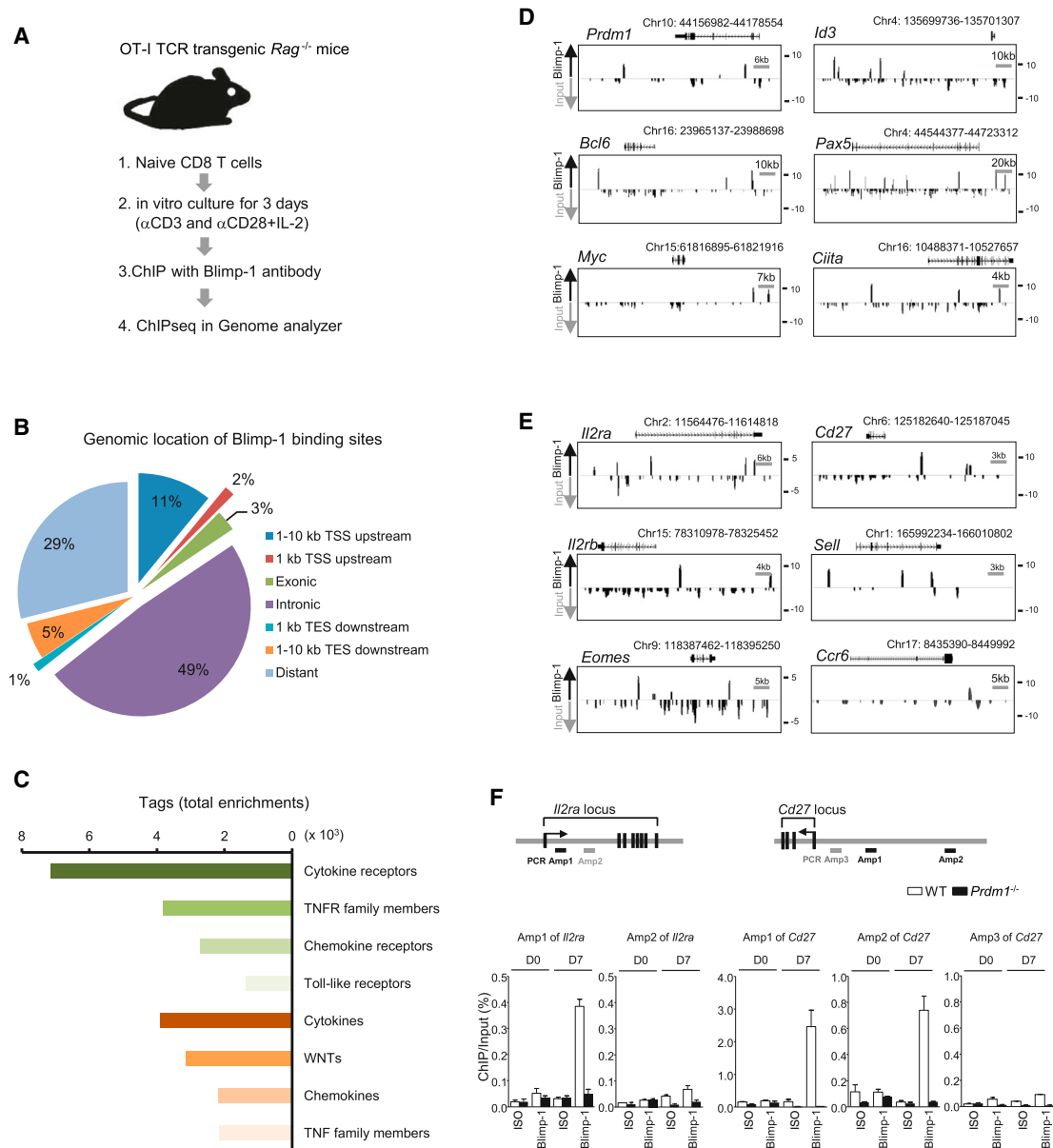


Figure 5. Genome-wide Identification of Blimp-1 Binding Sites in CD8⁺ T Cells

(A) Naive CD8⁺ T cells isolated from OT-I⁺*Rag1*^{-/-} mice were stimulated with plate-bound α CD3 and α CD28 and IL-2 (50ng/ml) for 3 days, and Blimp-1 ChIP-seq followed.

(B) Frequency (pie chart) of Blimp-1 binding sites localized to each region of target genes in the mouse genome (mm9). Abbreviations are as follows: TSS, transcription start site; and TES, transcription end site.

(C) Functional grouping of genes related to secreted proteins and their cognate receptors with Blimp-1 binding sites within 10 kb of the transcription start site.

(D and E) Identification of Blimp-1 binding sites on known (D) and unknown (E) target genes. The scale bars indicate the relative kb scale on each gene, and the numbers on the right display the magnitude of sequence enrichment on a log2 scale. Peaks were identified with Cisgenome 2.0, and all enrichment data on Blimp-1 binding sites are shown in the ChIP-seq tracks.

(F) WT and *Prdm1*^{-/-} mice were infected with LCMV, and CD44^{hi}CD8⁺ T cells were isolated at day 7 postinfection. As a control, naive CD8⁺ T cells were isolated from uninfected mice (D0). ChIP assays were performed with antibodies to Blimp-1 or mouse immunoglobulin G (IgG) (ISO). Each ChIP eluate was amplified by quantitative PCR (qPCR) for the indicated regions of *Il2ra* (PCR amplicons 1 and 2; left two panels) or *Cd27* (PCR amplicons 1, 2, and 3; right three panels). Amplicon 2 of *Il2ra* and amplicon 3 of *Cd27* indicate nonspecific regions where Blimp-1 binding was not detected by ChIP-seq. Data shown include a compilation of three independent experiments, and error bars represent the SEM.

See also Figure S4 and Table S1.

Immunity

Epigenetic Modification by Blimp-1 in CD8⁺ T Cells

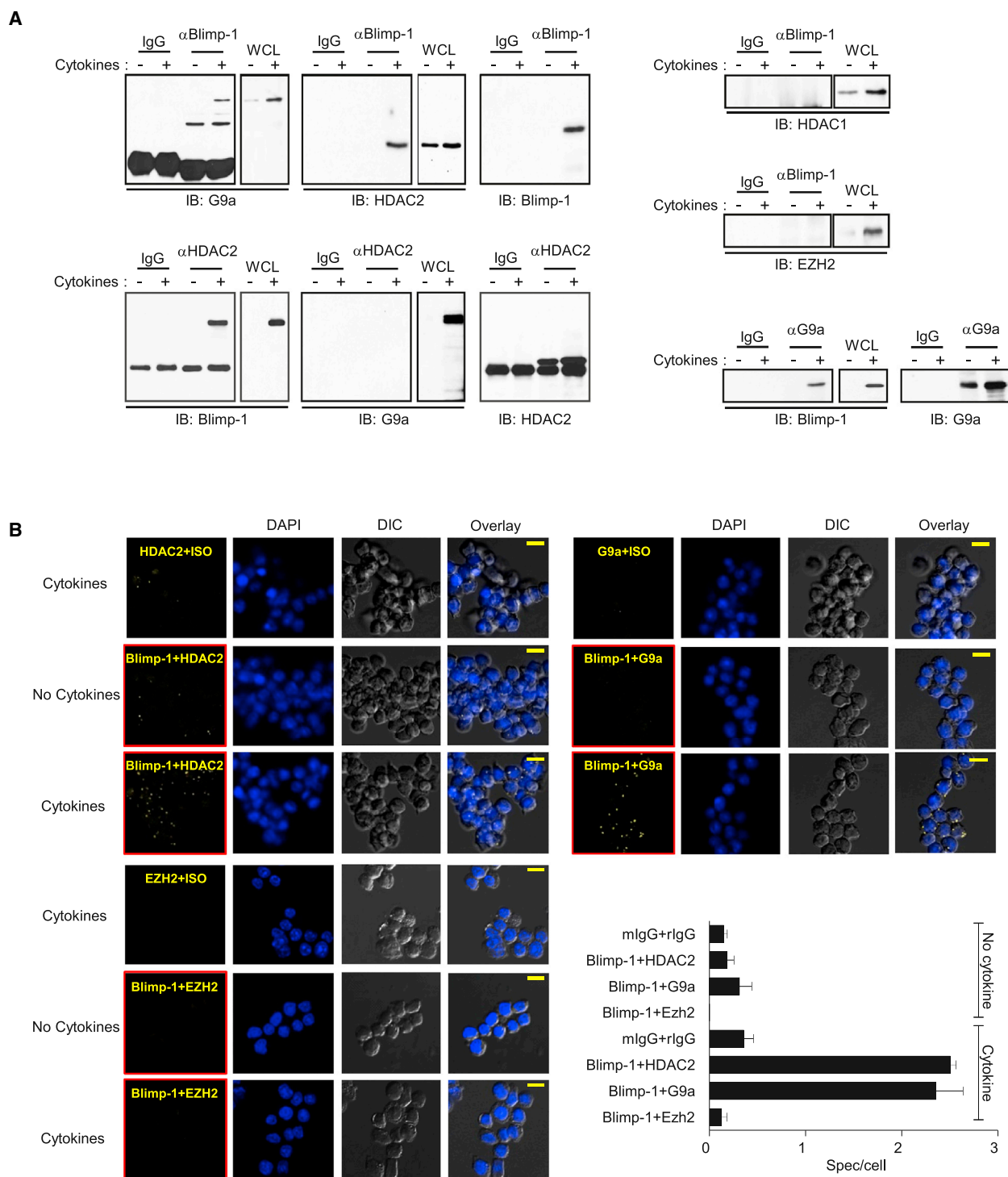


Figure 6. Blimp-1 Recruits G9a and HDAC2 in Activated CD8⁺ T Cells

(A) WT CD8⁺ T cells were stimulated in vitro with αCD3 and αCD28 for 2 days with (+) or without (–) a cocktail of cytokines containing IL-2, IL-4, and IL-12. Lysates were immunoprecipitated with αBlimp-1 (left top panels, right top panel, and middle panel), αHDAC2 (left bottom panels), or αG9a (right bottom panels) antibodies. Immunoblotting (IB) with the indicated antibodies followed. Data are representative of three independent experiments. The following abbreviation is used: WCL, whole-cell lysate.

(B) Stimulated CD8⁺ T cells were stained with (1) αHDAC2 and either a mouse IgG control (ISO) or αBlimp-1 (left upper panels), (2) αG9a and a mouse IgG control or αBlimp-1 (left lower panels), or (3) αEZH2 and a mouse IgG control or αBlimp-1 (left lower panels), and the Duolink proximity ligation assay followed. Samples were counterstained for nuclei (blue; DAPI). Yellow signals demonstrate close proximity of the two proteins. The graph (lower right panel) is a compilation of data from three independent experiments, and error bars represent the SEM.

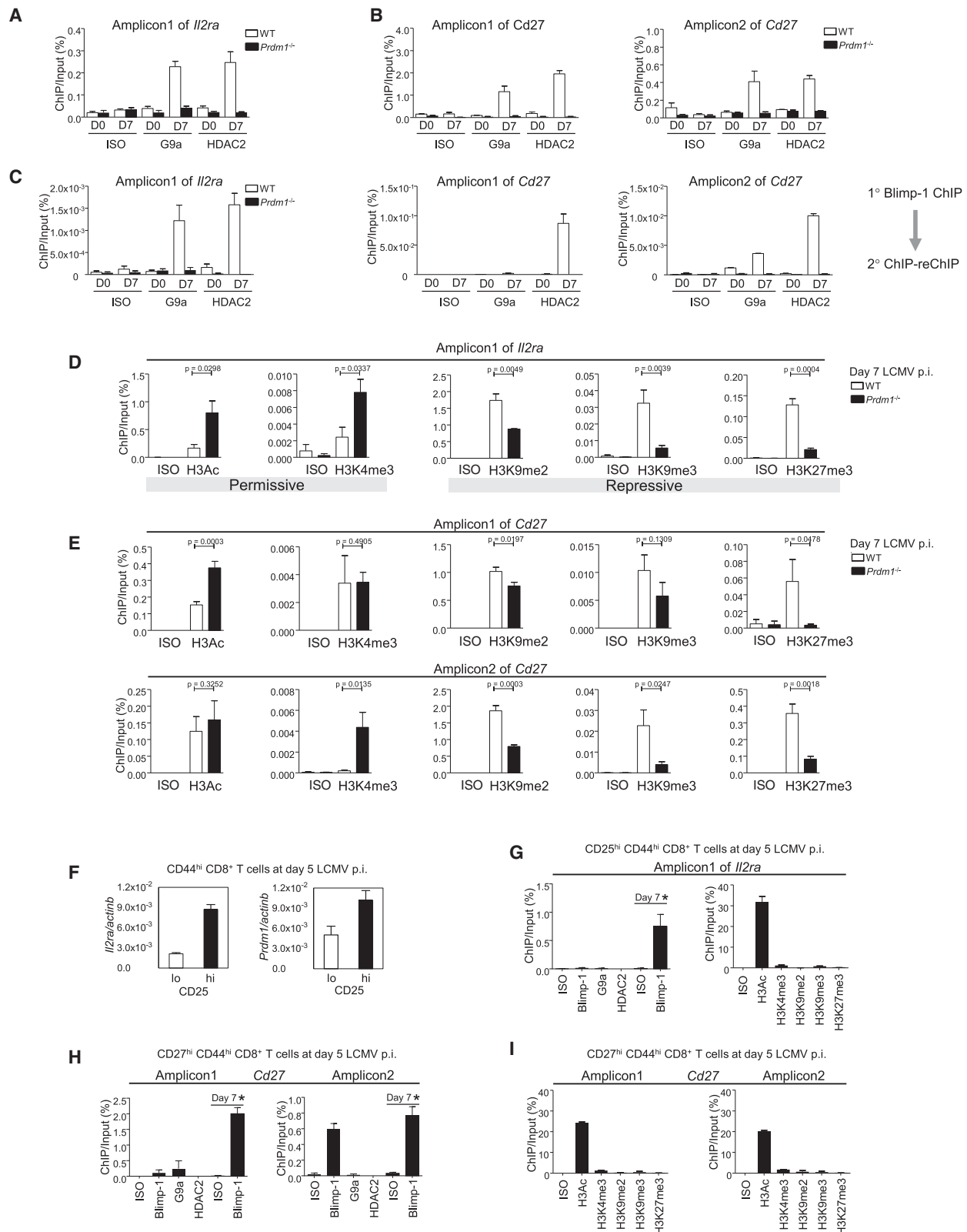


Figure 7. Blimp-1 Regulates Histone Modifications at the *Il2ra* and *Cd27* Loci in CD8⁺ T Cells at Day 7 after LCMV Infection

(A and B) WT and *Prdm1*^{-/-} mice were infected with LCMV, and CD44^{hi}CD8⁺ T cells were isolated at day 7 postinfection. As a control, naive CD8⁺ T cells were isolated from uninfected mice (D0). ChIP assays were performed with antibodies to G9a or HDAC2. Each ChIP eluate was amplified by qPCR for the indicated (legend continued on next page)

distinct mechanisms at different stages of the antiviral immune response, and further, whether the function of IL-2R signaling might also vary between T cell priming and T cell contraction. CD25 expression on CD8⁺ T cells is rapidly induced during the early stage of viral infection, mediated by a combination of TCR and IL-2R signaling (Boyman and Sprent, 2012). During this early stage, cells expressing CD25 are destined to be short-lived effectors, in keeping with their high Blimp-1 expression (Kalia et al., 2010; Rutishauser et al., 2009). Our data indicate that, at this time point, Blimp-1 expression is not able to override the positive signals promoting CD25 expression. In contrast, by day 7 postinfection, CD25 expression is nearly absent on virus-specific cells, a change that is Blimp-1 dependent. We propose that after viral clearance and the cessation of IL-2 production, CD25 expression becomes susceptible to regulation by Blimp-1. It has been shown previously that *Prdm1*^{-/-} mice consistently maintain higher proportions and numbers of memory CD8⁺ T cells (Rutishauser et al., 2009). Although we have not directly looked at later time points after viral infection, the transcription factor EOMES was upregulated in *Prdm1*^{-/-} mice, consistent with our ChIP-seq analysis. *Prdm1*^{-/-} mice were also more responsive to IL-15 stimulation. Therefore, it is likely that the EOMES and IL-15 axis promotes the homeostatic proliferation and survival of the increased memory T cell pool in *Prdm1*^{-/-} mice.

Here, we confirmed that CD25 and CD27 expression was significantly altered in *Prdm1*^{-/-} CD8⁺ T cells during the course of LCMV infection. Blimp-1 directly bound to the *Il2ra* locus, was required for recruitment of HDAC2 and G9a to this gene, and was required for the repressive chromatin modifications seen at the *Il2ra* locus in CD8⁺ T cells from day 7 LCMV-infected mice. The transcriptional regulation of *Il2ra* in response to TCR stimulation plus IL-2 has been well studied (Malek, 2008). Several transcription factors orchestrate this response, and four major regulatory regions have been identified (Kim et al., 2001; Malek, 2008). The first intron of the gene contains binding sites for signal transducer and activator of transcription 5a (STAT5a), STAT5b, and high-mobility group protein 1 (HMG-I(Y)), and binding of these factors occurs in response to IL-2 (Kim et al., 2001). Interestingly, it is this region that also contains the Blimp-1 binding site identified in our ChIP-seq analysis and verified by our Blimp-1 ChIP assays, further supporting a model in which Blimp-1-mediated repression of *Il2ra* is antagonistic to the positive signals upregulating *Il2ra* transcription.

Unlike that of *Il2ra*, the transcriptional regulation of *Cd27* is not well defined in T cells. Although present on naive T cells, TCR stimulation leads to further upregulation of CD27 (de Jong et al., 1991). The mechanisms leading to CD27 downregulation are even more poorly characterized. Although ligation with CD70 or stimulation with phorbol myrsitate acetate downregulates CD27 expression (Hintzen et al., 1994; Nolte et al., 2005), the factors mediating this event are not known. Our work has provided evidence that Blimp-1 plays a key role in CD27 downregulation following the peak of the antiviral CD8⁺ T cell response. As with the *Il2ra* locus, Blimp-1 binds to *Cd27* and recruits the histone-modifying enzymes, HDAC2 and G9a, leading to repressive modifications at this locus during CD8⁺ T cell contraction.

The histone-modifying enzyme G9a has recently been a topic of investigation in lymphocytes (Thomas et al., 2008). Although the development of lymphocytes in G9a-deficient mice was found to be normal, amounts of H3K9me2 were greatly reduced and led to aberrantly low usage of Igλ L chains in B cells (Thomas et al., 2008); in addition, G9a has been shown to regulate H3K9me3 in vivo (Collins and Cheng, 2010). More recently, G9a-deficient CD4⁺ T cells were shown to be impaired in cytokine production associated with T helper 2 cells and exhibited increased IL-17A and IFN-γ production, demonstrating that G9a regulates genes involved in lineage specification of CD4⁺ T cells (Lehnertz et al., 2010). Our data indicate that in virus-specific CD8⁺ T cells, Blimp-1 recruits HDAC2 and G9a to critical target genes that determine the fate of these T cells during the contraction of the immune response. Although it remains possible that Blimp-1 recruits additional chromatin-modifying enzymes not examined in our studies, our data clearly demonstrate that Blimp-1 plays a key role in regulating epigenetic marks that impact the balance of short-lived effector versus memory-precursor CD8⁺ T cells responding to acute virus challenge.

EXPERIMENTAL PROCEDURES

Mice

Mice were bred and housed in specific pathogen-free conditions at the University of Massachusetts Medical School (UMMS) in accordance with the guidelines of the Institutional Animal Care and Use Committee of UMMS. OT-I TCR transgenic *Rag1*^{-/-} mice were purchased from Taconic. WT C57BL/6 (CD90.2⁺CD45.2⁺) mice were purchased from Jackson Laboratories, and CD4-Cre mice were a gift from Joonsoo Kang at UMMS. *Prdm1*^{-/-} mice

region (PCR amplicon1) of *Il2ra* (A) or for each of two regions (PCR amplicon1 and amplicon2) of *Cd27* (B). Data shown include a compilation of three independent experiments.

(C) ChIP eluates from αBlimp-1 immunoprecipitates were reprecipitated with αG9a, αHDAC2, or rabbit IgG (isotype control [ISO]) antibodies. Secondary ChIP eluates were amplified by qPCR for the indicated regions of *Il2ra* and *Cd27*. Data shown include a compilation of three independent experiments.

(D and E) WT and *Prdm1*^{-/-} mice were infected with LCMV, and CD44^{hi}CD8⁺ cells were isolated at day 7 postinfection. ChIP assays were performed with antibodies to modified histone H3 as indicated. ChIP eluates were amplified by qPCR for the indicated regions of *Il2ra* (D) and *Cd27* (E). Two permissive (H3Ac and H3K4me3) and three repressive (dimethylated lysine 9 [H3K9me2], trimethylated lysine 9 [H3K9me3], and trimethylated lysine 27 [H3K27me3]) modifications of histone H3 were analyzed. Data shown include a compilation of three independent experiments.

(F) The mRNA expression of *Il2ra* and *Prdm1* in CD25^{hi}CD44^{hi}CD8⁺ or CD25^{lo}CD44^{hi}CD8⁺ T cells sorted at day 5 postinfection were analyzed by quantitative RT-PCR. Data shown include a compilation of three independent experiments.

(G–I) CD25^{hi}CD44^{hi}CD8⁺ T cells or CD27^{hi}CD44^{hi}CD8⁺ T cells were sorted at day 5 postinfection. ChIP assays were performed with antibodies to Blimp-1, G9a, HDAC2, or control IgG and with antibodies to modified histone H3 as indicated. For direct comparison, ChIP assays were performed with antibodies to Blimp-1 or control IgG on CD44^{hi}CD8⁺ T cells sorted at day 7 postinfection (G and H; D7*). Each ChIP eluate was amplified by qPCR for the indicated regions of *Il2ra* (G) and *Cd27* (H and I). Each graph is a compilation of data from three independent experiments, and error bars represent the SEM.

The following abbreviation is used: ISO, isotype control antibody.

have been described previously (Ohinata et al., 2005). Unless otherwise indicated, C57BL/6 CD4-Cre⁺ transgenic mice were used as WT controls. For some experiments, P14⁺Prdm1^{fl/fl} mice were crossed to Granzyme B-Cre⁺ transgenic mice for the deletion of Blimp-1 in activated CD8⁺ T cells, as previously described (Rutishauser et al., 2009).

T Cell Isolation and Adoptive Transfer

A total of 2×10^5 P14⁺CD45.1⁺ splenocytes were adoptively transferred into CD45.2⁺ recipient mice, and infection with LCMV followed. At day 7 postinfection, total CD8⁺ T cells were isolated with the CD8⁺ T Cell Isolation Kit (Miltenyi Biotec) and then CD25^{lo}P14⁺CD45.1⁺CD8⁺ or CD25^{hi}P14⁺CD45.1⁺CD8⁺ T cells were further sorted on a FACSria cell sorter. A total of 1×10^6 sorted cells were adoptively transferred into infection-matched CD45.2⁺ congenic WT mice. For CD27, 1×10^6 CD27^{lo}P14⁺CD45.1⁺CD8⁺ or CD27^{hi}P14⁺CD45.1⁺CD8⁺ T cells at day 9 postinfection were sorted on a FACSria and adoptively transferred into infection-matched CD45.2⁺ congenic WT mice. Recipient mice were analyzed at day 8 posttransfer for CD25 or day 7 posttransfer for CD27. The absolute numbers and percentages of P14⁺ cells were determined by staining with α -CD8, α -CD44, and α -CD45.1 antibodies.

Proximity Ligation Assay and Confocal Microscopy

CD8⁺ T cells were cytopun onto positively-charged microscope slides (Fisher, 12-550-20) and washed with cold PBS twice and were subsequently fixed with 4% paraformaldehyde at 25°C for 10 min. Fixed cells were washed with PBS twice and permeabilized in PBS with 0.5% Triton X-100 at 4°C for 6 min and were then washed with 70% ethanol. After samples were blocked in the proximity ligation assay (PLA) blocking solution for 30 min at 37°C, they were incubated at 4°C overnight with (1) α HDAC2 and either a mouse immunoglobulin G (IgG) control or α Blimp-1 (1:100 dilution), (2) α G9a and a mouse IgG control or α Blimp-1 (1:100 dilution), or (3) α EZH2 (1:100 dilution) and a mouse IgG control or α Blimp-1 (1:100 dilution); the Duolink proximity ligation assay was subsequently performed according to the manufacturer's instructions. Samples were counterstained for nuclei (blue; DAPI). The signals (red) from each pair of PLA probes were detected with laser-scanning confocal microscopy (Leica TCS SP5 II) with a 63 \times phase contrast oil immersion objective (numerical aperture = 1.3). The nuclei images were captured with the UV laser. Duolink Detection kit 613 (LNK-90133-30), Duolink PLA probe Mouse Plus (LNK-90701-30), and Duolink PLA probe Rabbit Minus (LNK-90602-30) were purchased from Olink bioscience.

CFSE Labeling and In Vitro T Cell Stimulation

CD8⁺ T cells were isolated from WT mice at days 5, 7, and 9 after LCMV infection or from WT, Prdm1^{fl/fl}, or Prdm1^{fl/fl} mice at day 7 postinfection. Cells were labeled with CFSE as previously described (Shi et al., 2009) and were cultured for 2 days with or without the indicated cytokines. IL-1 β , IL-6, IL-12, IL-18, IL-21, and IL-23 were purchased from R&D. IL-2 and IL-4 were purchased from BD Biosciences. IFN- γ , IL-7, and IL-15 were purchased from PeproTech. IFN- β was purchased from PBL Interferon Source. Cytokine concentrations were as follows: IFN- β (200 U), IFN- γ (200 U), IL-1 β (50 ng/ml), IL-2 (40 ng/ml), IL-4 (40 ng/ml), IL-6 (40 ng/ml), IL-7 (20 ng/ml), IL-12 (20 ng/ml), IL-15 (20 ng/ml), IL-18 (20 ng/ml), IL-21 (20 ng/ml), and IL-23 (40 ng/ml).

Statistical Analysis

The statistical difference between samples was analyzed with an unpaired Student's t test. All error bars in this report represent the SEM.

ACCESSION NUMBERS

The Blimp-1 ChIP-seq data are available in the Gene Expression Omnibus (GEO) database (<http://www.ncbi.nlm.nih.gov/gds>) under the accession number GSE48358.

SUPPLEMENTAL INFORMATION

Supplemental Information includes Supplemental Experimental Procedures, four figures, one table, and Supplemental References and can be found with this article online at <http://dx.doi.org/10.1016/j.immuni.2013.08.032>.

ACKNOWLEDGMENTS

We thank A. Tarakhovsky for Prdm1 floxed mice, S.L. Nutt for Blimp-1-GFP mice, and R.T. Woodland for the contribution of mice. We thank members of the Berg and Welsh labs for technical assistance and helpful discussions. We thank O.H. Cho and R. Rohatgi for helpful discussions and critical reading of the manuscript. We also thank Flow Cytometry Core Lab and Deep Sequencing Core facility at UMMS. This work was supported by NIH grants AI084987 (L.J.B.), AI017672 (R.M.W.) and AI081675 (R.M.W.), AI074699 (S.M.K.), and HHMI (S.M.K.).

Received: June 12, 2012

Accepted: June 24, 2013

Published: October 10, 2013

REFERENCES

- Ancelin, K., Lange, U.C., Hajkova, P., Schneider, R., Bannister, A.J., Kouzarides, T., and Surani, M.A. (2006). Blimp1 associates with Prmt5 and directs histone arginine methylation in mouse germ cells. *Nat. Cell Biol.* 8, 623–630.
- Araki, Y., Wang, Z., Zang, C., Wood, W.H., 3rd, Schones, D., Cui, K., Roh, T.Y., Lhotsky, B., Wersto, R.P., Peng, W., et al. (2009). Genome-wide analysis of histone methylation reveals chromatin state-based regulation of gene transcription and function of memory CD8⁺ T cells. *Immunity* 30, 912–925.
- Banerjee, A., Gordon, S.M., Intlekofer, A.M., Paley, M.A., Mooney, E.C., Lindsten, T., Wherry, E.J., and Reiner, S.L. (2010). Cutting edge: The transcription factor eomesodermin enables CD8⁺ T cells to compete for the memory cell niche. *J. Immunol.* 185, 4988–4992.
- Blattman, J.N., Grayson, J.M., Wherry, E.J., Kaech, S.M., Smith, K.A., and Ahmed, R. (2003). Therapeutic use of IL-2 to enhance antiviral T-cell responses in vivo. *Nat. Med.* 9, 540–547.
- Boyman, O., and Sprent, J. (2012). The role of interleukin-2 during homeostasis and activation of the immune system. *Nat. Rev. Immunol.* 12, 180–190.
- Collins, R., and Cheng, X. (2010). A case study in cross-talk: the histone lysine methyltransferases G9a and GLP. *Nucleic Acids Res.* 38, 3503–3511.
- de Jong, R., Loenen, W.A., Brouwer, M., van Emmerik, L., de Vries, E.F., Borst, J., and van Lier, R.A. (1991). Regulation of expression of CD27, a T cell-specific member of a novel family of membrane receptors. *J. Immunol.* 146, 2488–2494.
- Doering, T.A., Crawford, A., Angelosanto, J.M., Paley, M.A., Ziegler, C.G., and Wherry, E.J. (2012). Network analysis reveals centrally connected genes and pathways involved in CD8⁺ T cell exhaustion versus memory. *Immunity* 37, 1130–1144.
- Dolfi, D.V., Boesteanu, A.C., Petrovas, C., Xia, D., Butz, E.A., and Katsikis, P.D. (2008). Late signals from CD27 prevent Fas-dependent apoptosis of primary CD8⁺ T cells. *J. Immunol.* 180, 2912–2921.
- Duttagupta, P.A., Boesteanu, A.C., and Katsikis, P.D. (2009). Costimulation signals for memory CD8⁺ T cells during viral infections. *Crit. Rev. Immunol.* 29, 469–486.
- Gong, D., and Malek, T.R. (2007). Cytokine-dependent Blimp-1 expression in activated T cells inhibits IL-2 production. *J. Immunol.* 178, 242–252.
- Gyory, I., Wu, J., Fejér, G., Seto, E., and Wright, K.L. (2004). PRDI-BF1 recruits the histone H3 methyltransferase G9a in transcriptional silencing. *Nat. Immunol.* 5, 299–308.
- Hendriks, J., Gravestien, L.A., Tesselaar, K., van Lier, R.A., Schumacher, T.N., and Borst, J. (2000). CD27 is required for generation and long-term maintenance of T cell immunity. *Nat. Immunol.* 1, 433–440.
- Hikono, H., Kohlmeier, J.E., Takamura, S., Wittmer, S.T., Roberts, A.D., and Woodland, D.L. (2007). Activation phenotype, rather than central- or effector-memory phenotype, predicts the recall efficacy of memory CD8⁺ T cells. *J. Exp. Med.* 204, 1625–1636.
- Hintzen, R.Q., Lens, S.M., Beckmann, M.P., Goodwin, R.G., Lynch, D., and van Lier, R.A. (1994). Characterization of the human CD27 ligand, a novel member of the TNF gene family. *J. Immunol.* 152, 1762–1773.

- Ji, Y., Pos, Z., Rao, M., Klebanoff, C.A., Yu, Z., Sukumar, M., Reger, R.N., Palmer, D.C., Borman, Z.A., Muranski, P., et al. (2011). Repression of the DNA-binding inhibitor Id3 by Blimp-1 limits the formation of memory CD8⁺ T cells. *Nat. Immunol.* 12, 1230–1237.
- Joshi, N.S., Cui, W., Chande, A., Lee, H.K., Urso, D.R., Hagman, J., Gapin, L., and Kaech, S.M. (2007). Inflammation directs memory precursor and short-lived effector CD8⁺ T cell fates via the graded expression of T-bet transcription factor. *Immunity* 27, 281–295.
- Kalia, V., Sarkar, S., Subramaniam, S., Haining, W.N., Smith, K.A., and Ahmed, R. (2010). Prolonged interleukin-2Rα expression on virus-specific CD8⁺ T cells favors terminal-effector differentiation in vivo. *Immunity* 32, 91–103.
- Kallies, A., Hawkins, E.D., Belz, G.T., Metcalf, D., Hommel, M., Corcoran, L.M., Hodgkin, P.D., and Nutt, S.L. (2006). Transcriptional repressor Blimp-1 is essential for T cell homeostasis and self-tolerance. *Nat. Immunol.* 7, 466–474.
- Kallies, A., Xin, A., Belz, G.T., and Nutt, S.L. (2009). Blimp-1 transcription factor is required for the differentiation of effector CD8⁺ T cells and memory responses. *Immunity* 31, 283–295.
- Kim, H.P., Kelly, J., and Leonard, W.J. (2001). The basis for IL-2-induced IL-2 receptor α chain gene regulation: importance of two widely separated IL-2 response elements. *Immunity* 15, 159–172.
- Kouzarides, T. (2007). Chromatin modifications and their function. *Cell* 128, 693–705.
- Kubicek, S., O'Sullivan, R.J., August, E.M., Hickey, E.R., Zhang, Q., Teodoro, M.L., Rea, S., Mechtler, K., Kowalski, J.A., Homon, C.A., et al. (2007). Reversal of H3K9me2 by a small-molecule inhibitor for the G9a histone methyltransferase. *Mol. Cell* 25, 473–481.
- Lehnertz, B., Northrop, J.P., Antignano, F., Burrows, K., Hadidi, S., Mullaly, S.C., Rossi, F.M., and Zaph, C. (2010). Activating and inhibitory functions for the histone lysine methyltransferase G9a in T helper cell differentiation and function. *J. Exp. Med.* 207, 915–922.
- Malek, T.R. (2008). The biology of interleukin-2. *Annu. Rev. Immunol.* 26, 453–479.
- Martins, G., and Calame, K. (2008). Regulation and functions of Blimp-1 in T and B lymphocytes. *Annu. Rev. Immunol.* 26, 133–169.
- Martins, G.A., Cimmino, L., Shapiro-Shelef, M., Szabolcs, M., Herron, A., Magnusdottir, E., and Calame, K. (2006). Transcriptional repressor Blimp-1 regulates T cell homeostasis and function. *Nat. Immunol.* 7, 457–465.
- Martins, G.A., Cimmino, L., Liao, J., Magnusdottir, E., and Calame, K. (2008). Blimp-1 directly represses IL2 and the IL2 activator Fos, attenuating T cell proliferation and survival. *J. Exp. Med.* 205, 1959–1965.
- Mitchell, D.M., Ravkov, E.V., and Williams, M.A. (2010). Distinct roles for IL-2 and IL-15 in the differentiation and survival of CD8⁺ effector and memory T cells. *J. Immunol.* 184, 6719–6730.
- Nolte, M.A., Arens, R., van Os, R., van Oosterwijk, M., Hooibrink, B., van Lier, R.A., and van Oers, M.H. (2005). Immune activation modulates hematopoiesis through interactions between CD27 and CD70. *Nat. Immunol.* 6, 412–418.
- Obar, J.J., and Lefrançois, L. (2010). Memory CD8⁺ T cell differentiation. *Ann. N Y Acad. Sci.* 1183, 251–266.
- Ohinata, Y., Payer, B., O'Carroll, D., Ancelin, K., Ono, Y., Sano, M., Barton, S.C., Obukhanych, T., Nussenzweig, M., Tarakhovsky, A., et al. (2005). Blimp-1 is a critical determinant of the germ cell lineage in mice. *Nature* 436, 207–213.
- Peperzak, V., Veraar, E.A., Keller, A.M., Xiao, Y., and Borst, J. (2010a). The Pim kinase pathway contributes to survival signaling in primed CD8⁺ T cells upon CD27 costimulation. *J. Immunol.* 185, 6670–6678.
- Peperzak, V., Xiao, Y., Veraar, E.A., and Borst, J. (2010b). CD27 sustains survival of CTLs in virus-infected nonlymphoid tissue in mice by inducing auto-crine IL-2 production. *J. Clin. Invest.* 120, 168–178.
- Pipkin, M.E., Sacks, J.A., Cruz-Guilloty, F., Lichtenheld, M.G., Bevan, M.J., and Rao, A. (2010). Interleukin-2 and inflammation induce distinct transcriptional programs that promote the differentiation of effector cytolytic T cells. *Immunity* 32, 79–90.
- Piskurich, J.F., Lin, K.I., Lin, Y., Wang, Y., Ting, J.P., and Calame, K. (2000). BLIMP-1 mediates extinction of major histocompatibility class II transactivator expression in plasma cells. *Nat. Immunol.* 1, 526–532.
- Razvi, E.S., Jiang, Z., Woda, B.A., and Welsh, R.M. (1995). Lymphocyte apoptosis during the silencing of the immune response to acute viral infections in normal, lpr, and Bcl-2-transgenic mice. *Am. J. Pathol.* 147, 79–91.
- Rutishauser, R.L., Martins, G.A., Kalachikov, S., Chande, A., Parish, I.A., Meffre, E., Jacob, J., Calame, K., and Kaech, S.M. (2009). Transcriptional repressor Blimp-1 promotes CD8⁺ T cell terminal differentiation and represses the acquisition of central memory T cell properties. *Immunity* 31, 296–308.
- Sarkar, S., Kalia, V., Haining, W.N., Konieczny, B.T., Subramaniam, S., and Ahmed, R. (2008). Functional and genomic profiling of effector CD8 T cell subsets with distinct memory fates. *J. Exp. Med.* 205, 625–640.
- Shi, M., Lin, T.H., Appell, K.C., and Berg, L.J. (2009). Cell cycle progression following naive T cell activation is independent of Jak3/common gamma-chain cytokine signals. *J. Immunol.* 183, 4493–4501.
- Shin, H., Blackburn, S.D., Intlekofer, A.M., Kao, C., Angelosanto, J.M., Reiner, S.L., and Wherry, E.J. (2009). A role for the transcriptional repressor Blimp-1 in CD8⁺ T cell exhaustion during chronic viral infection. *Immunity* 31, 309–320.
- Smith, M.A., Wright, G., Wu, J., Taylor, P., Ozato, K., Chen, X., Wei, S., Piskurich, J.F., Ting, J.P., and Wright, K.L. (2011). Positive regulatory domain 1 (PRDM1) and IRF8/PU.1 counter-regulate MHC class II transactivator (CIITA) expression during dendritic cell maturation. *J. Biol. Chem.* 286, 7893–7904.
- Su, S.T., Ying, H.Y., Chiu, Y.K., Lin, F.R., Chen, M.Y., and Lin, K.I. (2009). Involvement of histone demethylase LSD1 in Blimp-1-mediated gene repression during plasma cell differentiation. *Mol. Cell. Biol.* 29, 1421–1431.
- Thomas, L.R., Miyashita, H., Cobb, R.M., Pierce, S., Tachibana, M., Hobeika, E., Reth, M., Shinkai, Y., and Oltz, E.M. (2008). Functional analysis of histone methyltransferase g9a in B and T lymphocytes. *J. Immunol.* 181, 485–493.
- Weng, N.P., Araki, Y., and Subedi, K. (2012). The molecular basis of the memory T cell response: differential gene expression and its epigenetic regulation. *Nat. Rev. Immunol.* 12, 306–315.
- Williams, M.A., Tyznik, A.J., and Bevan, M.J. (2006). Interleukin-2 signals during priming are required for secondary expansion of CD8⁺ memory T cells. *Nature* 441, 890–893.
- Yu, J., Angelin-Duclos, C., Greenwood, J., Liao, J., and Calame, K. (2000). Transcriptional repression by blimp-1 (PRDI-BF1) involves recruitment of histone deacetylase. *Mol. Cell. Biol.* 20, 2592–2603.